

Thin film fracture: Ti-coating–Be-substrate bond failure

A. F. JANKOWSKI

Rockwell International, North American Space Operations, PO Box 464, Golden, Colorado 80402-0464, USA

The role of microstructure in the fracture of the bond between vapour-deposited thin film coatings and substrates will be modelled to a first approximation using classical fracture mechanics principles. Vapour-deposited coatings are composed of a grain structure with varying orientations. The effect of differing degrees of texture on the bond strength between the coating and its substrate will be considered in this analysis. Incorporated in stress calculations will be the residual stresses arising from the thermal contraction of the coating, an applied tensile stress normal to the coating surface (as that in an adherence pull test) and the critical stress needed for coating–substrate bond failure.

1. Introduction

The applied load necessary to induce bond failure, that is fracture of the bonded interface, is in part a function of the state of stress existing in the as-deposited coating–substrate system. Intergranular fracture results when the effective planar stress, the stress in the plane of the coating, exceeds a critical value. This critical stress necessary to induce fracture is greater than superimposed residual planar stresses which result from the thermal contraction of the coating's variously oriented grains. When the applied load normal to the surface is sufficiently large (greater than the existing normal component of residual thermal stress in the coating) fracture then occurs.

In this study, titanium-coated beryllium substrates will be considered in the fracture analysis. Coatings with varying degrees of texture were produced by altering the deposition variables of substrate temperature (350 to 550°C) and coating rate (2.8 to 24.0 nm sec⁻¹) in the physical vapour deposition of titanium on as-machined beryllium coupon blanks [1]. A correlation between a low (0002) texture of the titanium coating and low bond strength of the coating to its substrate was previously found [1]. The analysis to follow will clarify the physical explanation behind this observation.

2. Theory

The planar stress required for fracture, the critical stress σ_c , has been modelled for a crack in a plate under uniform tension by Griffith [2], using an energy balance approach. For a coating–substrate system, the sudden rupture of the coating to substrate bond under an applied load is representative of a brittle two-dimensional medium (with the coating) in a state of plane strain. In this analysis, the stress applied to the coating–substrate bond (needed to induce failure) must be greater than the residual thermal stress in the coating which arose during deposition.

The coating–substrate system will be subjected to a

tensile load applied normal to its surface. This can be modelled, as shown in Fig. 1, by applying a load to a pull stud (with a surface diameter d) epoxied to the coating surface. The state of stress in this system is shown in Fig. 2, assuming the coating (of thickness 30.5 μm) is under a state of plane strain [1]. The planar stress in the coating surface, σ_r , may be related to the stress normal to its surface, σ_z , by the relation [3]

$$\sigma_z = \nu \sigma_r \quad (1)$$

where ν is the coating's Poisson ratio (ν for titanium is equivalent to 0.36 [4]). The load applied to the pull stud yields the applied normal stress

$$\sigma^a = P/A \quad (2)$$

where, P is the applied load and A is the pull stud contact area which equals $\frac{1}{4}\pi d^2$. (An aluminium pull stud is used with a 0.254 cm diameter [1]). The applied normal stress in the pull stud, σ^a , can be related to the surface normal stress at the coating–substrate interface by using a stress concentration factor k ,

$$\sigma_z = k\sigma^a \quad (3)$$

The stress concentration factor for a microcracked coating–substrate interface, in a state of plane strain, may be approximated with a value of 2 using fracture mechanics principles [5]. The applied load can then be related to the coating planar stress σ_r using Equations 1 and 3,

$$\sigma^a = 2\sigma_r/\nu \quad (4)$$

The coating planar stress σ_r^a required for coating–substrate bond failure must exceed the value arising from residual thermal (contractive) stresses, σ^T , during deposition. The critical condition for fracture is therefore

$$\sigma_r^a + \sigma^T > 0 \quad (5a)$$

or equivalently using Equations 4 and 5a

$$\frac{1}{2}\nu\sigma^T + \sigma^a > 0 \quad (5b)$$

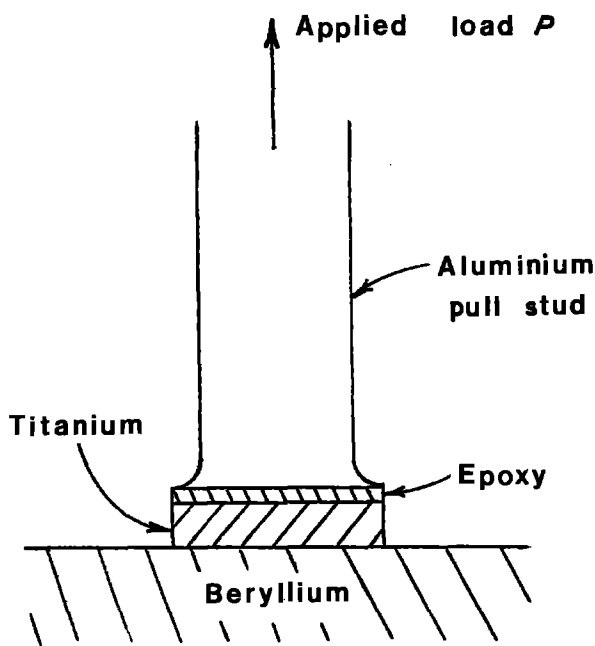


Figure 1 A schematic diagram of the adherence test. An aluminum pull stud is epoxied normal to the coating surface.

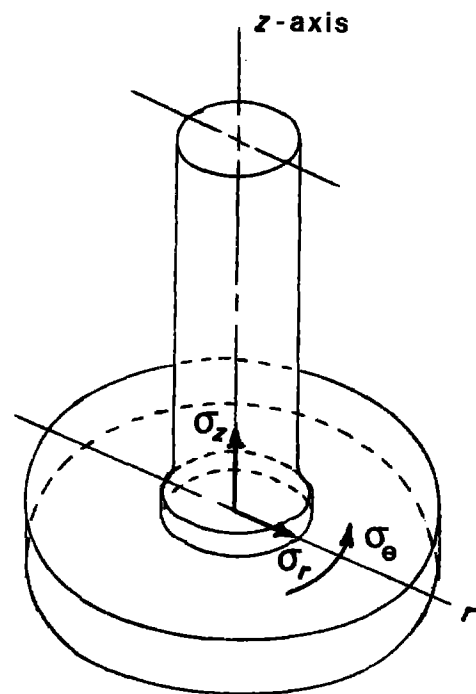


Figure 2 A schematic diagram of the cylindrical coordinate stress axes system referenced in the fracture analysis. Assume; $\sigma_z \neq 0$, $\sigma_r \neq 0$, $\sigma_\theta = 0$.

Equation 5a represents the planar inequality for fracture and Equation 5b the surface normal inequality for fracture.

The planar residual thermal stress in the coating is due to the thermal contraction of the coating (from elevated temperatures during deposition to testing at room temperature). The coatings are composed of grains of varying orientations, hence varying degrees of texture. The planar residual thermal stress, σ^T , can therefore be theoretically computed based on the coating texture. Each differently oriented grain has unique values for its elastic moduli [6] and thermal expansion coefficients [7-9]. The planar stress attributable to a grain of orientation $(hkl)_i$ is simply

$$\sigma_i^T = \int_{T_d}^{T_r} (\alpha_i E_i) dT \quad (6)$$

where α_i is the $(hkl)_i$ thermal expansion coefficient dependence on temperature, E_i is the $(hkl)_i$ Young's modulus dependence on temperature, T_d is the deposition temperature and T_r is room temperature.

The relative proportion of each grain orientation within the coating can be computed utilizing an inverse pole figure calculation based on measured X-ray intensities of the diffracted beam [1]. The frac-

tional composition of each $(hkl)_i$ grain orientation, c_i , may be expressed as

$$c_i = \frac{T_{ci}}{\sum_{i=1}^n T_{ci}} \quad (7)$$

where T_{ci} is the calculated degree of texture of the $(hkl)_i$ intensity reflection with respect to a random powder file intensity value and $i = 1, 2, \dots, n$. The net state of planar residual thermal stress, σ^T , in the coating attributable to all $(hkl)_i$ grains, can then be approximated as an arithmetic summation of each σ_i^T contribution

$$\sigma^T = \sum_{i=1}^n c_i \sigma_i^T = c_i \sigma_i^T \quad (8)$$

The critical stress condition for fracture, Equations 5a and 5b, may now be computed theoretically and compared to the value obtained experimentally.

3. Theoretical results

The dependence of coating texture on deposition rate and substrate temperature is illustrated in Tables I and

TABLE I Selected low texture $T_c(hkl)$ titanium coatings

Sample number	Deposition variables		Texture $T_c(hkl)$									
	T (°C)	Rate (nm sec ⁻¹)	1010	0002	1011	1012	1120	1013	1122	2021	1014	2023
1	400	14	0.6	1.3	1.8	1.1	0.3	1.3	1.3	0.5	0	1.8
48	400	14	0	0.4	1.4	1.9	0	1.6	0.8	0	2.4	1.5
109	400	14	0.3	0.7	1.4	2.3	0	0.8	0.9	0	0	3.8
30	450	14	0.4	1.7	1.3	0.7	0.3	0.9	1.0	0.9	1.7	1.2
40	450	14	1.5	0.9	1.1	1.1	3.3	0.5	0.8	0.8	0	0
54	450	14	1.9	0.5	2.2	0.9	1.3	0	1.1	0.9	0	1.4
111	500	24	0.6	0.6	1.0	1.9	0.4	0.8	1.7	0	0	3.1

TABLE II Selected high texture $T_c(hkil)$ titanium coatings

Sample number	Deposition variables		Texture $T_c(hkil)$									
	T ($^{\circ}\text{C}$)	Rate (nm sec^{-1})	10 $\bar{1}$ 0	0002	10 $\bar{1}$ 1	10 $\bar{1}$ 2	11 $\bar{2}$ 0	10 $\bar{1}$ 3	11 $\bar{2}$ 2	20 $\bar{2}$ 1	10 $\bar{1}$ 4	20 $\bar{2}$ 3
110	400	24	0	6.3	0	1.2	0.1	0.5	0	0	0.8	1.1
17	450	14	0.1	6.4	1.3	0.8	0	0.2	0	0.1	0.9	0.3
8	500	14	0.4	2.6	5.7	0.3	0.2	0.3	0.5	0	0	0
112	500	14	0.2	1.8	3.7	2.6	0.2	0.4	0	0.5	0	0.6
31	550	2.8	0.1	4.7	2.5	1.6	0	0.3	0	0.3	0	0.5
33	550	14	0	8.3	0.7	0.6	0	0.1	0	0.1	0	0.1

II for titanium-coated beryllium substrates. High and low texture values of selected coatings to be pull tested are listed.

Mathematical expressions for the dependence of elastic constants C_{ij} and elastic moduli in crystallographic system and orientation are well known [10]. The temperature dependence of the individual titanium elastic constants C_{ij} [6] and the dependence of Young's modulus on both orientation and temperature (seen in Table III) is quite clear. For example, at a room temperature of 25°C , the $E(0002)$ is 40% greater than $E(10\bar{1}0)$.

The dependence of the thermal expansion coefficient on both orientation and temperature is evidenced in the following equations derived from experimental data [7-9]

$$\alpha[0002] = [9.1 + (0.0063 T)] \times 10^{-6}/^{\circ}\text{C} \quad (9)$$

$$\alpha[10\bar{1}0] = [7.4 + (0.0053 T)] \times 10^{-6}/^{\circ}\text{C} \quad (10)$$

The planar residual thermal stress can be calculated for any coating by combining: (i) the relative composition of the oriented grains within each coating (Equation 7, Tables I and II); (ii) the temperature and orientation dependence of Young's modulus (Table III); with (iii) the temperature and orientation dependence of the thermal expansion coefficients. The thermal stress for each $(hkil)$, σ_i^T (see Equation 6), is then represented by the following equation with the corresponding coefficients, Γ_i , in Table IV,

$$\sigma_i^T = \Gamma_1 \times 10^5 T + \Gamma_2 \times 10^2 T^2 + \Gamma_3 \times 10^{-1} T^3 \quad (\text{Pa}) \quad (11)$$

The planar residual thermal stress, σ^T , can now be calculated for the titanium coatings. Results of these calculations are listed in Table V. The resolved surface normal component is tabulated as well for comparison to the applied tensile stress required for coating-substrate bond failure (Equation 5b).

4. Experimentation and results

A uniaxial tension test was utilized for the coating-substrate bond failure analysis. Two types of testing procedures were used. A Sebastian Adherence Test [1] was limited by an upper test stress equivalent to 68.9 MPa (10 k.s.i.). An adherence bonding pull stud is epoxied perpendicular to the $30.5 \mu\text{m}$ (1.2 mil) thick titanium coating, as shown in Fig. 1. The remaining exposed titanium is then machined away. The bonding test has a contact surface diameter of 0.254 cm (0.100 in). The tensile test is performed by applying load to the pull stud while the attached coupon is held stationary. For titanium-beryllium bond stresses less than 68.9 MPa this test is adequate. However, for bond fracture stresses above 68.9 MPa and less than 84.7 MPa (the epoxy yield stress) a second testing procedure was devised [11]. An Instron Tester was employed with a machined aluminium tee-slot fixture (universally mounted) to hold the beryllium coupon substrate (0.508 cm thick with a 2.54 cm diameter) and a tubular steel clamp to hold the epoxied pull stud. A strain rate of $8.47 \mu\text{m sec}^{-1}$ and a load range of 890 N provided fracture measures equivalent to those measured using the Sebastian Adherence Tester. Results for the normal fracture stress, σ^a , of the vapour-deposited titanium-coated (as machined) beryllium substrates are listed in Table V.

5. Analysis of results

A comparison of the normal stress applied through the pull stud to induce coating-substrate bond fracture, σ^a , and that theoretically calculated from the residual thermal stress, $\frac{1}{2}\nu\sigma^T$, appears in Table V. The correspondence between these values is quite remarkable considering the simplification of the fracture analysis in this study. Coating-substrate bond failures were correctly predicted for all the samples observed to fail in this mode (below the epoxy bond strength of 84.7 MPa). Epoxy bond failures coincided with all the

TABLE III Young's modulus of titanium dependence on orientation and temperature

Temperature $T(^{\circ}\text{C})$	$E(hkil)$ (TPa)*										
	10 $\bar{1}$ 0	0002	10 $\bar{1}$ 1	10 $\bar{1}$ 2	11 $\bar{2}$ 0	10 $\bar{1}$ 3	11 $\bar{2}$ 2	20 $\bar{2}$ 1	10 $\bar{1}$ 4	20 $\bar{2}$ 3	
25	0.104	0.143	0.117	0.130	0.104	0.136	0.124	0.108	0.139	0.125	
300	0.079	0.130	0.100	0.117	0.079	0.123	0.109	0.086	0.126	0.110	

* (Pa) $\times 1.450377 \times 10^{-6} = (\text{p.s.i.})$

TABLE IV Thermal stress equation coefficients

<i>i</i>	$\Gamma_i(hkil)$									
	10 $\bar{1}0$	0002	10 $\bar{1}1$	10 $\bar{1}2$	11 $\bar{2}0$	10 $\bar{1}3$	11 $\bar{2}2$	20 $\bar{2}1$	10 $\bar{1}4$	20 $\bar{2}3$
1	7.89	13.1	9.85	10.9	7.89	11.4	10.4	9.16	11.6	10.5
2	-0.583	2.41	0.828	1.72	-0.583	1.99	1.34	-0.107	2.09	1.41
3	-1.63	-0.990	-1.22	-0.976	-1.63	-0.930	-1.01	-1.54	-0.920	-1.05

samples with theoretical values greater than 84.7 MPa. The actual fracture stress was predicted within $8 \pm 2\%$ for five of the six coating-substrate failures.

Those coatings with high (0002) texture did indeed manifest high bond strengths as represented by epoxy failures rather than coating-substrate bond failures. This experimental observation is supported by the residual thermal stress calculation. This high (0002) texture to high bond strength correlation is directly attributable to the higher elastic modulus which exists for (0002), as shown in Table III. In addition to high (0002) texture, a high deposition temperature will also increase bond strength. In general, the convolution of the percentage increase in thermal contraction with increased deposition temperature is greater than the percentage decrease in elastic modulus accompanying increased deposition temperature. The lowest bond strengths would be predicted and were experimentally observed for low (i.e. random) textured coatings deposited at low temperatures.

The contribution of electrostatic adhesive bonding appears to minimal for the titanium coatings on the as-machined beryllium substrates. For atomically smooth interfaces this result would most probably not be the case. The increase in surface contact area for atomically smooth surfaces would be expected to increase the contribution from the surface smoothness dependence of electrostatic adhesive bonding [12-15]. The roughness of the as-machined substrate surface, however, is essential for the surface interlocking bonding mechanism of thermal residual stress bonding [16-18].

A third factor to consider, in addition to the electrostatic and residual thermal adhesive bonding stresses, is the tensile strength of the coating. If the

resolved planar stress of the applied load exceeds the tensile stress of the coating before the coating to substrate bonding stress is reached, the mechanism of failure will be the fracture of the titanium coating. As a result of the excess titanium coating being machined away from the pull stud prior to tensile testing, this mechanism is not possible. The remaining coating surface is entirely supported by the pull stud epoxy.

6. Summary

The role of microstructure in the bond failure of vapour-deposited titanium coatings from beryllium substrates has been modelled using basic fracture mechanics principles. The effect of the varying textures of each coating on bond strength has been incorporated into a residual thermal stress calculation. The model developed proved successful in identifying those samples with a coating-substrate bond failure. Bond strength is shown to increase with high (0002) texture, as previously postulated [1], and in general with increased deposition temperature.

Acknowledgements

I would like to thank Dr C. Heiple for his constructive comments and suggestions during the preparation of this manuscript.

References

1. A. F. JANKOWSKI, "Ti-Be Residual Strain Analysis: Role of Deposition Variables on Texture and Strength", Rockwell International Rocky Flats Publication 3926 (1986) 24 pages.
2. A. A. GRIFFITH, *Phil. Trans. R. Soc. A* 221 (1920) 163.
3. R. G. BUDYNAS, "Advanced Strength and Applied Stress Analysis", (McGraw-Hill, New York, 1977) p. 30.
4. G. F. CARTER, "Mechanical, Physical and Chemical

TABLE V Titanium-beryllium bond fracture stress

Sample number	Coating residual thermal stress		Experimental normal fracture stress, σ^a (MPa)
	Theoretical planar, $\sigma^T = c_i \sigma_i^T$ (GPa)	Resolved normal, $\frac{1}{2} \nu \sigma^T$ (MPa)	
1	-0.409	-73.7	+68.2
48	-0.433	-77.9	+31.7
109	-0.424	-76.5	+80.6
39	-0.484	-86.8	+77.2
40	-0.395	-71.0	+75.1
54	-0.415	-74.4	+79.9
110	-0.490	-88.2	epoxy*
17	-0.555	-99.9	epoxy
8	-0.524	-94.4	epoxy
112	-0.533	-100.6	epoxy
111	-0.521	-93.7	epoxy
31	-0.644	-115.7	epoxy
33	-0.736	-132.3	epoxy

*Epoxy fracture stress $\sigma^a = 84.7 \pm 2.1$ (MPa). Critical condition for bond failure $\frac{1}{2} \nu \sigma^T + \sigma^a > 0$ (Equation 5b).

- Properties of Metals", ASM Metals Handbook (ASM, Metals Park, Ohio, 1985) p. 2.16.
5. R. E. PETERSON, "Stress Concentration Factors" (Wiley, New York, 1974).
 6. E. S. FISHER and C. J. RENKEN, *Phys. Rev.* **135** (1964) A482.
 7. A. D. McQUILLAN and M. K. McQUILLAN, "Titanium", (Academic Press, New York, 1956) p. 139.
 8. R. L. P. BERRY and G. V. RAYNOR, *Research, Lond.* **6** (1953) 21S.
 9. E. S. GREINER and W. C. ELLIS, *Trans. Amer. Inst. Min. (Metall.) Engrs.* **180** (1949) 657.
 10. J. F. NYE, "Physical Properties of Crystals", (Clarendon Press, Oxford, 1960) p. 131.
 11. S. BEITSCHER and A. JANKOWSKI, unpublished research, January 1986.
 12. K. L. MITTAL, "Adhesion Measurement: Recent Progress, Unsolved Problems, and Prospects", Adhesion Measurement of Thin Films, Thick Films, and Bulk Coatings (ASTM STP 640, 1978) pp. 5-17.
 13. Z. V. SHELKUNOVA and S. V. GEGIN, "Electrostatic Method of Evaluating Adhesion Forces on Refractory Metals", *Zavodskaya Laboratoriya* No. 6 (1976) 708-9.
 14. B. V. DERYAGUIN, *Research* **8** (1955) 70.
 15. H. CZICHOS, *J. Phys. D: Appl. Phys.* **5** (1972) 1890.
 16. G. A. HERPOL and E. TAVERNIER, *Brit. Welding J.* (1966) 683.
 17. J. W. DINI and H. R. JOHNSON, *Metal Finishing* **3** (1977) 42.
 18. W. D. BASCOM and J. L. BITNER, *J. Mater. Sci.* **12** (1977) 1401.

*Received 27 February
and accepted 22 May 1986*